RSC Advances

PAPER

View Article Online
View Journal | View Issue

Check for updates

Cite this: *RSC Adv.*, 2020, **10**, 28186

Rapid and facile method to prepare oxide precursor solution by using sonochemistry technology for WZTO thin film transistors†

Yanyu Yuan, Cong Peng, Shibo Yang, Meng Xu, Jiayu Feng, Xifeng Li* and Jianhua Zhang

Received 15th June 2020
Accepted 20th July 2020

DOI: 10.1039/d0ra05245k

rsc.li/rsc-advances

In this paper, a rapid and facile method of preparing metal-oxide semiconductor precursor solution using sonochemistry technology is proposed. Compared with the traditional method (water bath above 60 °C for several hours), the efficiency of preparing solution is improved, because sonochemical reaction is found to accelerate the dissolution of solutes and the agitation of solution. The color comparison and thermal gravimetric and differential scanning calorimetry of solution confirme the formation of W-doped zinc tin oxide (WZTO) precursor solution with good performance. The effects of sonochemical reactions on the film structure, surface morphology, optical properties and chemical composition of WZTO thin films are analyzed by atomic force microscopy, X-ray diffraction, UV visible spectrum and X-ray photoelectron spectroscopy. The results show that the film has a smooth surface, an amorphous structure, a high transmittance and more M–O bonding. Hence, a rapid process of preparing WZTO solution (sonochemical treatment for 10 min) and fabricate TFT with high electron mobility (2.7 $cm^2 V^{-1} s^{-1}$) is established, while the corresponding mobility of the traditional method is 1.2 $cm^2 V^{-1} s^{-1}$. The results show that the sonochemical reaction can improve the efficiency of preparing solution by 1800% and it is a fast and efficient method for preparing precursor solutions.

Open Access Article. Published on 28 July 2020. Downloaded on 8/15/2024 10:14:40 PM.
This article is licensed under a Creative Commons Attribution-NonCommercial 3.0 Unported Licence.

1. Introduction

In recent years, amorphous oxide semiconductors (AOSs) and silicon-based thin film transistors (TFTs) have had commercial applications in flat panel displays. In particular, AOS TFTs have become potential substitutes for organic and silicon materials in thin film transistors due to their high carrier mobility and excellent large area uniformity.[1–4] Among the various manufacturing processes of AOS TFTs, printing technology instead of the conventional vacuum process has provided an attractive way to fabricating TFTs because of low cost, facile process, and low power consumption.[5–9] The key factor to promote the development of printing AOS TFT technology is the stable and high-performance precursor solution to fabricate TFT.[10–13] At present, the formation of precursor solution involves several key steps: the decomposition of the metal alkoxide in an organic solvent, formation of the homogeneous solution, and formation of gel at a certain temperature. These processes involve hydrolysis and condensation chemical reactions in the solution, thus affording the M–O–M frameworks.[11,14–18] It requires high temperature and long-time water bath treatment (above 60 °C for several hours) and agitation, which remarkably increases the cost of time and waste of resources.[19–22] Therefore, it is urgent to develop a rapid and high-effective method for preparing precursor solution. Fortunately, we find that sonochemical reaction can accelerate the dissolution of solutes and the solution agitation and does not require additional heating conditions.[23–25] With sonochemical reactions, cavitation bubbles will form in the solution, and the turbulence, growth, shrinkage and rupture of cavitation bubbles will trigger physical and chemical changes. So it is very interesting and attractive to try applying the sonochemical reaction to form metal-oxide semiconductor precursor solution, which is significant for the future development of the printing-electronic industry.

Among the most studied MOS, zinc tin oxide (ZTO) TFTs have high carrier mobility and high light transmittance, ZTO is cost-effective by replacing indium oxide semiconductor.[26–30] However, there are several obstacles in ZTO TFTs, such as bias, light and thermal stress.[31–33] Recent studies have shown that solution process can be uniformly and quantitatively doped at the molecular level to solve these issues.[34–36] Our previous study suggested tungsten (W) ions plays a leading role in changing the performance of the ZTO film and the stability of the TFT thanks to the W element as an oxygen vacancies suppressor.

In this paper, we have tried and successfully developed a rapid and facile method for preparing uniform and steady

Key Laboratory of Advanced Display and System Applications of Ministry of Education, Shanghai University, Shanghai 200072, P. R. China. E-mail: lixifeng@shu.edu.cn

† Electronic supplementary information (ESI) available. See DOI: 10.1039/d0ra05245k

This journal is © The Royal Society of Chemistry 2020

Open Access Article. Published on 28 July 2020. Downloaded on 8/15/2024 10:14:40 PM.
This article is licensed under a Creative Commons Attribution-NonCommercial 3.0 Unported Licence.

precursor solution by sonochemical reaction in a few minutes. The method avoids the high temperature, long-time water bath treatment in the conventional solution process and improve the efficiency of preparing solution by 1800%. We analyze the effect of sonochemical reaction on WZTO solution, films and TFTs thoroughly, discuss the role of sonochemical reaction and verify that it is a fast and efficient method for preparing metal-oxide precursor solution.

2. Experimental section

2.1 Preparation of metal oxide solution

A 0.3 M WZTO precursor was synthesized by dissolving tungsten hexachloride (WCl_6, Alfa Aesar, 99%), zinc acetate dihydrate ($Zn(CH_3COO)_2 \cdot 2H_2O$, SIGMA, 98%) and chloride pentahydrate ($SnCl_4 \cdot 5H_2O$, SIGMA, 98%) into 2-methoxy ethanol (2-MOE). 2-MOE is usually used as a solvent because it acts as a bridging ligand and stabilizes the intermediate-high molecular weight oligomer. In addition, 0.3 M monoethanolamine (MEA) was added for long-term solution stability. The atomic ratio of W : Sn : Zn in the solution was fixed at 1 : 30 : 70. All chemicals were used as received without further purification.

Fig. 1 presents the schematic of an ultrasound device. The entire ultrasonic device consists of three parts, including an ultrasonic generator, a high-power ultrasonic transducer, and an ultrasonic probe. The ultrasonic probe was immersed into a solution container, in which case the ultrasonic waves propagated in the solution and accelerated the dissolution of solutes and the agitation of solution. The sonochemical treatment was at a frequency of 20 kHz and at a power of 300 W.

2.2 Device fabrication

TFTs were fabricated on thermally grown 100 nm silicon dioxide layers on a silicon wafer (Si/SiO_2), which was used as bottom-gate electrode/dielectric, respectively. The silicon wafer was cleaned sequentially in deionized water, acetone, and isopropanol with ultrasonic bath for 10 min. After the ultrasonic bath, in order to remove the residual solvents, the sample was heated at 100 °C for 10 min in an oven heated and then the sample was exposed to ultraviolet ozone for 10 min. Thereafter, the WZTO solution was filtered on the sample through a 0.22 μm polytetrafluoroethylene (PTFE) syringe filter and then spin-coated on it at 3000 rpm for 30 s. After that, the samples were soft-annealed at 200 °C for 10 min and then post-annealed at 500 °C for 1 h. Finally, Al electrodes were deposited onto the top of the active layer as source/drain electrodes by thermal evaporation. The TFT channel width and length were 700 μm and 70 μm, respectively.

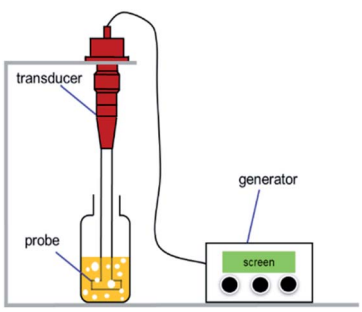

Fig. 1 Schematic configuration diagram of ultrasonic system, including an ultrasonic generator, a high-power ultrasonic transducer, and an ultrasonic probe.

2.3 Measurement and analysis

The thermal behavior of the WZTO solution monitored under atmosphere by thermal gravimetric and differential scanning calorimetry (TG-DSC, SDT Q600) which was operated at temperatures ranging from room temperature to 800 °C at a scan rate of 10 °C min^{-1}. The surface topography and roughness of WZTO films were analyzed by atomic force microscopy (AFM, Nanonavi SPA-400 SPM). The optical properties and absorption spectra were characterized by UV-visible spectrometer (H-3900, Hitachi). The crystallization information of WZTO films was obtained by incidence X-ray diffraction (XRD, D/MAX-2550) with a glancing incident angle of 1°. The film thickness and refractive index were measured by spectroscopic ellipsometry (M-2000DI). The chemical bonding of the oxygen and metal ions that form the WZTO films were examined by X-ray photoelectron spectroscopy (XPS, Thermo ESCALAB 250XL). The chemical structure of the WZTO films was analyzed by Fourier transform infrared spectroscopy (FTIR, Nicolet 380). The electrical measurement of the TFTs was carried out using a semiconductor characterization system (Keithley, Model 4200-SCS) and a microprobe station (Cascade Microtech, Model Summit-11600 AP) at room temperature in the dark.

3. Results and discussion

With the increase of time, the color of WZTO precursor solutions during the sonochemical experiment are shown in ESI Fig. S1.† It can be seen that cavitation bubbles appear immediately as soon as sonochemical treatment starts. With the procession of sonochemical reactions, cavitation bubbles will form in the solution, and the turbulence, growth, shrinkage and rupture of cavitation bubbles will trigger physical and chemical changes, and these reactions can accelerate the dissolution of solutes and the agitation of solution.[37–39] After a few minutes, the color of precursor solution changes from colorless to pale yellow, which demonstrates the formation of precursor solution. As the time increased, the solution turns yellow. ESI Fig. S2† shows the color comparison by different treatment ways. Some of them show a lighter color, for example water bath 1 h solution, sonochemical treatment 3 min solution and sonochemical treatment 5 min solution. This may be due to the incomplete alcoholization of the solution. All solutions were also clear and transparent and can be kept clean in the air for more than a week. The color change of the sonochemical solution from 3 min to 10 min and water bath solution from 1 h to 3 h are the same, the fact denotes that the formation time of precursor solution using sonochemistry technology decreases even 3 times more than that by traditional method, and

Open Access Article. Published on 28 July 2020. Downloaded on 8/15/2024 10:14:40 PM.
This article is licensed under a Creative Commons Attribution-NonCommercial 3.0 Unported Licence.

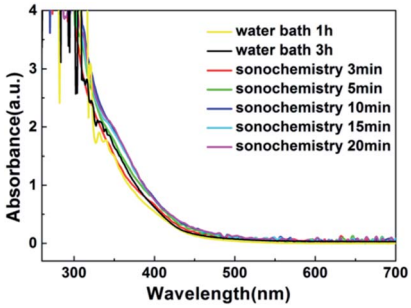

Fig. 2 Schematic configuration diagram of ultrasonic system, including an ultrasonic generator, a high-power ultrasonic transducer, and an ultrasonic probe.

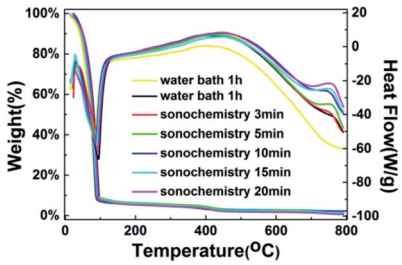

Fig. 3 Thermal gravimetric and differential scanning calorimetry (TG-DSC) curves of WZTO precursors.

indicates that the efficiency of preparing solution was greatly improved by 1800%.

Fig. 2 shows the ultraviolet-visible absorption spectrum of WZTO precursor solution with different sonochemical and water bath treatment time. It can be found that the absorption spectra of the two types of solutions are almost the same. After the sonochemical treatment time exceeds 10 min, there is almost no change in absorption, indicating that stable precursor solution has been formed for only 10 min. It implies that it is feasible to form the precursor solution with sonochemical treatment.

Fig. 3 shows the TG-DSC curves of the WZTO precursor with different sonochemical and water bath treatment time to examine the thermal behavior of the WZTO solution, TG-DSC analysis is performed under air atmosphere from room temperature to 800 °C. The chemical reaction is divided into three stages. The first endothermic reaction is observed in the range below 90 °C. The weight loss is large, which is typically caused by the evaporation of the solvent. A wide exothermic peak is observed in the range of 380–450 °C, and its weight loss is slight. This corresponds to the behavior of gradual condensation, forming a metal–oxygen–metal (M–O–M) framework, reducing the impurities in the film and making the film denser. Since no visible weight loss was noticed in all samples after 500 °C, the oxidation behavior of the WZTO was almost accomplish. TGA results indicate that 500 °C is an acceptable annealing temperature for WZTO film formation.

Fig. 4 shows the AFM image of WZTO films with different sonochemical and water bath treatment time. All films are

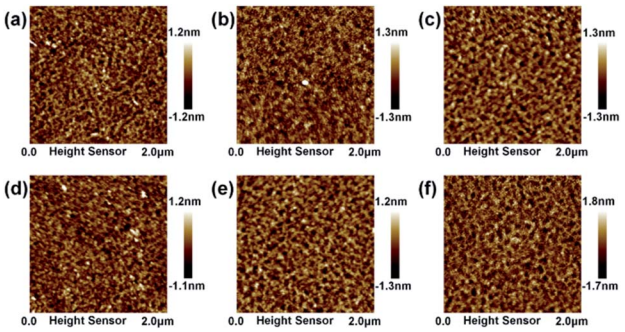

Fig. 4 AFM images of WZTO films with water bath time as (a) 3 h, and different sonochemical treatment time as (b) 3 min, (c) 5 min, (d) 10 min, (e) 15 min and (f) 20 min.

annealed at 500 °C. The root mean square (RMS) roughness value is calculated from the AFM image. The RMS values of WZTO with sonochemical treatment time of 3 min, 5 min, 10 min, 15 min, and 20 min are 0.31 nm, 0.30 nm, 0.24 nm, 0.40 nm, and 0.41 nm, respectively. All WZTO films show uniform smooth surface with an RMS roughness value of less than 1 nm. The RMS roughness (0.27 nm) of the water bath WZTO film is also analyzed, which is comparable to the RMS roughness of the WZTO films obtained from the sonochemical solution. This phenomenon indicates that the WZTO films obtained by the sonochemical solution has a smooth surface. The phenomenon further strengthens the evidence that the sonochemical reaction is an effective way to form and obtain the oxide semiconductor precursor solution.

Fig. 5 shows the XRD image of WZTO films with different sonochemical treatment and water bath time. No significant crystallization peak is observed in all WZTO films prepared by different solution, and only a wide halo peak located near 32° is observed. It implies that the WZTO films prepared by traditional water bath method and the films using sonochemistry technique are all amorphous. The amorphous phase of the WZTO films may contribute to the formation of a smooth surface WZTO film and uniform properties of TFT devices, which is very much consonant with the AFM results. And it may be advantageous for the manufacture of considerable oxide TFTs.

The optical transmittance characteristics of the WZTO films are measured to identify the effect of the solution preparation method on the films. The cleaned glass substrate is used as

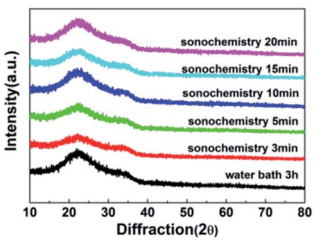

Fig. 5 XRD pattern of the various WZTO samples obtained by different methods.

This journal is © The Royal Society of Chemistry 2020

Open Access Article. Published on 28 July 2020. Downloaded on 8/15/2024 10:14:40 PM.
This article is licensed under a Creative Commons Attribution-NonCommercial 3.0 Unported Licence.

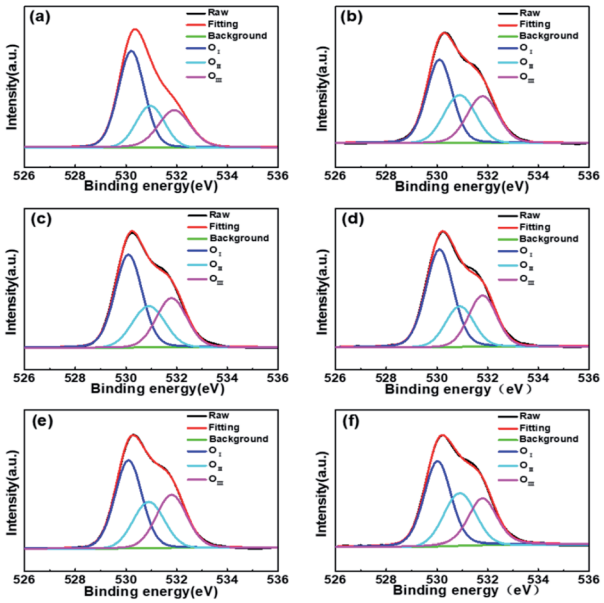

Fig. 6 X-ray photoelectron spectroscopy (XPS) spectra of O 1s peaks for the WZTO films with (a) water bath treatment for 3 h, (b) sonochemical treatment for 3 min, (c) sonochemical treatment for 5 min, (d) sonochemical treatment for 10 min, (e) sonochemical treatment for 15 min, and (f) sonochemical treatment for 20 min.

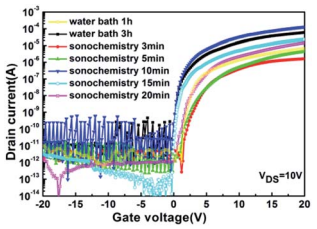

Fig. 7 Transfer characteristics (I_{DS}–V_{GS}) of the WZTO TFT device with different treatments of precursor solution.

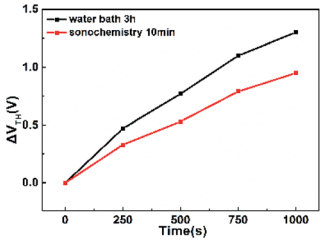

Fig. 8 Shift of threshold voltage as a function of the stress time under the positive gate bias stress (PBS) for the WZTO TFTs, including the samples with sonochemical treatment for 10 min and water bath treatment for 3 h.

a sample reference during the measurement. All WZTO films have relatively high optical transmittance in the visible light region (greater than 85%), indicating that the solution obtained by sonochemical treatment has no apparent effect on transparency (optical transmission is shown in ESI Fig. S3†).

We further compare the refractive index (n) dispersion curves to verify the densification behavior of the WZTO films by a spectroscopic ellipsometer measurement (refractive index image is shown in ESI Fig. S4†). At a wavelength of 550 nm, the refractive index of the film prepared by the solution obtained by sonochemical treatment for 10 min is 1.78, which is equivalent to the value of the corresponding film obtained by water bath for 3 h, these high refractive indices are comparable to those of vacuum-deposited films.

ESI Fig. S5† shows the FTIR spectra of different WZTO TFTs. Several peaks are observed in WZTO thin films. According to group theory, the broad peak between 3000 and 3500 cm^{-1} is related to –OH stretching modes. Two sharp peaks at about 2921 and 2853 cm^{-1} are consistent with the symmetric and asymmetric $-CH_3$ stretching vibrations. Besides, many –OH and asymmetric C=O groups are presented, which could suppress the densifying of the WZTO thin film by chelating with coordination bonding to the metal elements.[40,41]

Fig. 6 shows the oxygen 1s (O 1s) XPS spectrum of different WZTO films. The carbon 1s peak at 284.6 eV is used as a reference for calibration in the XPS results. It can be decomposed into three peaks of 530.1 ± 0.2 eV (peak 1), 530.9 ± 0.2 eV (peak 2) and 531.8 ± 0.2 eV (peak 3), respectively. The O 1s peak confirms the details of the oxidation behavior of the WZTO films with different sonochemical treatment and water bath time. Previous studies have shown that the peak at 530 eV (peak

Table 1 Summary of the proportion of different oxygen binding states of the WZTO films. [*i.e.* $O_I/(O_I + O_{II} + O_{III})$, $O_{II}/(O_I + O_{II} + O_{III})$, $O_{III}/(O_I + O_{II} + O_{III})$]

	O_I (%)	O_{II} (%)	O_{III} (%)
Water bath 3 h	51.8%	23.1%	25.1%
Sonochemistry 3 min	43.4%	28.3%	28.3%
Sonochemistry 5 min	48.6%	23.9%	27.5%
Sonochemistry 10 min	52.0%	21.5%	26.5%
Sonochemistry 15 min	44.8%	25.3%	29.9%
Sonochemistry 20 min	44.2%	28.9%	26.9%

Table 2 Comparison of the device performance for WZTO TFT with water bath treatment and sonochemical treatment

	μ ($cm^2\ V^{-1}\ s^{-1}$)	V_{TH} (V)	SS (V dec^{-1})	I_{on}/I_{off}
Water bath 1 h	0.12	3.3	0.41	7.5×10^5
Water bath 3 h	1.22	1.4	0.14	1.2×10^6
Sonochemistry 3 min	0.05	3.6	0.22	1.1×10^6
Sonochemistry 5 min	0.11	4.6	0.28	1.6×10^6
Sonochemistry 10 min	2.70	1.2	0.14	5.1×10^7
Sonochemistry 15 min	0.43	1.5	0.17	4.3×10^6
Sonochemistry 20 min	0.25	2.6	0.34	7.3×10^6

Open Access Article. Published on 28 July 2020. Downloaded on 8/15/2024 10:14:40 PM.
This article is licensed under a Creative Commons Attribution-NonCommercial 3.0 Unported Licence.

Table 3 Comparison on the various solution-processed oxide semiconductors with different methods for preparing precursor

Material	Process method	Temperature	Process time	Reference
ZTO	Magnetically stir	Room temperature	12 h	42
ITO	Water bath	75 °C	12 h	43
Li:NiO_x	Water bath	60 °C	2 h	44
IZO	Water bath	70 °C	12 h	45
In_2O_3	Water bath	90 °C	12 h	19
WZTO	Sonochemistry technology	Room temperature	10 min	This work

1) corresponds to lattice oxygen in a perfectly coordinated environment, while the peak at higher binding energy near 531 eV (peak 2) is derived from an anoxic environment. The highest binding energy peak of (peak 3) is most likely related to the O–H bond in the adsorbed water molecule, because the M–OH oxygen atom has a negative charge in the oxide, which leads to a shift to higher binding energy. Solution-processed metal oxide films typically have two kinds of different defects: (1) defects induced by organic chemistry, including organic residues, pores, and pinholes; (2) inherent lattice defects such as oxygen vacancies. Table 1 summarizes the different oxygen bonding states of the WZTO samples. It can be observed that as the sonochemical reaction time increases, the M–O concentration of the WZTO film increases from 43.4% to the highest of 52.0% at 10 min, and then decreases to only 44.2% at 20 min. The M–O concentration of the WZTO film prepared by sonochemical solution for 10 min is slightly higher than that of the film through water bath for 3 h. Hosono *et al.* shows that the conduction band minimum in metal oxide semiconductors is mainly composed of dispersed vacancy states to achieve efficient carrier transport.[2] The M–O–M framework in the metal oxide acts as an electron conduction path, while the M–OH and oxygen vacancies act as trap sites, impeding charge transport. This implies that the chemical structure composed of less hydroxides and oxygen vacancies with more metal–oxygen bonding in precursor solutions, would improve the device performance. From our results, it is the best processing condition to treat the solution by sonochemical treatment for 10 min.

Fig. 7 shows the transfer characteristics of different WZTO TFTs. At room temperature, the drain-to-source voltage (V_{DS}) is fixed at 10 V and the gate voltage (V_{GS}) is varied between −20 and 20 V. The mobility (μ), the threshold voltage (V_{TH}), the subthreshold swing (SS), and the ratio of the on-state current to the off-state current (I_{on}/I_{off}) are extracted according to the transmission curve and are summarized in Table 2. We can see that even if the sonochemical treatment time is reduced to 10 min, the performance of the TFTs are significantly improved compared to that in the water bath for 3 h, the mobility is 2.7 $cm^2\ V^{-1}\ s^{-1}$ and 1.2 $cm^2\ V^{-1}\ s^{-1}$, respectively. However, WZTO TFTs prepared with solutions below 10 min show much lower mobility ($\mu = 0.11\ cm^2\ V^{-1}\ s^{-1}$). This is due to the fact that the solutions are not fully alcoholized because they are not completely discolored. This leads to low M–O bond affects the process of electron transport, as shown in the XPS results. After the sonochemical reaction time exceeds 10 min, the performance of the TFT is relatively poor. Since the treatment time is long, sonochemical reaction results in more M–O bond breaks and more M–OH and oxygen vacancy defects, which are confirmed in the XPS results. This means that sonochemical treatment requires optimal time. When we reduced the bath time to 1 h, the performance of the WZTO TFTs show very poor mobility ($\mu = 0.12\ cm^2\ V^{-1}\ s^{-1}$). This is same to the performance of TFT prepared by the solution obtained by sonochemical treatment for 5 min, but the time is reduced by more than ten times. This shows that the precursor solution obtained by sonochemical reaction greatly shortens the experiment time and improves the performance of the TFT device.

Fig. 8 shows the positive gate bias stress (PBS) test results of device. We measured the PBS of WZTO TFT at a sufficient forward bias of 5 V at room temperature to verify the operational stability of the WZTO TFT in air under dark conditions, at a gate voltage (V_{GS}) of ±20 V, a drain voltage (V_{DS}) of 10 V. We can see that the WZTO TFT prepared by the sonochemical solution fabricated on the silicon substrate has excellent operational stability even without device packaging or passivation. After the gate bias stress time is 1000 s, the V_{TH} offset (ΔV_{TH}) is very small, 0.95 V. It is superior to the WZTO TFT prepared by the 3 h water bath solution (1.3 V). This indicates that the optimal sonochemical time promotes conversion to WZTO semiconductor, and the WZTO solution prepared by sonochemical treatment for 10 min effectively suppresses the oxygen vacancies of the WZTO film, which is also confirmed by XPS data. Therefore, the WZTO solution prepared by sonochemical treatment can improve the stability of the TFT. This further confirms that the sonochemical method is an efficient method for preparing a solution, and can effectively improve the performance of the WZTO TFT device. Table 3 presents the reported solution precursor oxide semiconductors with different methods for preparing precursor. Based on detailed comparisons between sonochemical treatment and other technology, it can be seen that sonochemical treatment is a high-effective method to prepare metal-oxide semiconductor precursor solution.

4. Conclusions

It is demonstrated that sonochemical treatment is a rapid and high-effective method preparing metal-oxide semiconductor precursor solution for thin-film transistor. The WZTO film prepared by sonochemistry technology is amorphous and has

 This journal is © The Royal Society of Chemistry 2020

Open Access Article. Published on 28 July 2020. Downloaded on 8/15/2024 10:14:40 PM.
This article is licensed under a Creative Commons Attribution-NonCommercial 3.0 Unported Licence.

a smooth surface. What's more, the film suppresses the formation of oxygen-related defects and provide strong M–O bonding. The sonochemical reaction can accelerate the dissolution of solutes and the agitation of solution. Therefore, the performance of WZTO TFTs are considerably enhanced even if the sonochemical treatment time is reduced to 10 min, and the efficiency of the reaction is improved 1800%. As a result, compared with the solution in water bath for 3 h, the device prepared from the precursor solution treated under sonochemical conditions for 10 min exhibited mobility and on–off current ratio increase from 1.2 to 2.7 $cm^2 V^{-1} s^{-1}$ and from 10^6 to 10^7, respectively. The V_{TH} shift caused by positive bias stress decreased from 1.3 to 0.95 V within 1000 seconds. Thus, sonochemical treatment is very suitable for the rapid production of solutions for practical applications, and shows great promise in the future.

Conflicts of interest

The authors declare no competing financial interest.

Acknowledgements

This work is supported by the National Key Research and Development Program of China under grant no. 2016YFB0401105, the National Natural Science Foundation of China under grant 61674101, Program of Shanghai Academic/Technology Research Leader under grant 18XD1424400, and the Shanghai Science and Technology Commission under grant 17DZ2291500. This work is also sponsored by "Shuguang Program" supported by Shanghai Education Development Foundation and Shanghai Municipal Education Commission under grant 18SG38.

References

1 S. Hong, J. W. Park, H. J. Kim, Y.-g. Kim and H. J. Kim, *J. Inf. Disp.*, 2016, **17**, 93–101.
2 K. Nomura, H. Ohta, A. Takagi, T. Kamiya, M. Hirano and H. Hosono, *Nature*, 2004, **432**, 488–492.
3 S. J. Lim, S.-j. Kwon, H. Kim and J.-S. Park, *Appl. Phys. Lett.*, 2007, **91**, 183517.
4 A. Suresh and J. F. Muth, *Appl. Phys. Lett.*, 2008, **92**, 033502.
5 A. C. Arias, J. D. MacKenzie, I. McCulloch, J. Rivnay and A. Salleo, *Chem. Rev.*, 2010, **110**, 3–24.
6 H. Sirringhaus, *Adv. Mater.*, 2005, **17**, 2411–2425.
7 H. Yan, Z. Chen, Y. Zheng, C. Newman, J. R. Quinn, F. Dotz, M. Kastler and A. Facchetti, *Nature*, 2009, **457**, 679–686.
8 J. H. Cho, J. Lee, Y. Xia, B. Kim, Y. He, M. J. Renn, T. P. Lodge and C. D. Frisbie, *Nat. Mater.*, 2008, **7**, 900–906.
9 Y. Y. Noh, N. Zhao, M. Caironi and H. Sirringhaus, *Nat. Nanotechnol.*, 2007, **2**, 784–789.
10 M. Li, W. Zhang, W. Chen, M. Li, W. Wu, H. Xu, J. Zou, H. Tao, L. Wang, M. Xu and J. Peng, *ACS Appl. Mater. Interfaces*, 2018, **10**, 28764–28771.
11 K. K. Banger, Y. Yamashita, K. Mori, R. L. Peterson, T. Leedham, J. Rickard and H. Sirringhaus, *Nat. Mater.*, 2011, **10**, 45–50.
12 T. S. Jung, H. Lee, H. J. Kim, J. H. Lee and H. J. Kim, *ACS Appl. Mater. Interfaces*, 2018, **10**, 44554–44560.
13 M. G. Kim, H. S. Kim, Y. G. Ha, J. He, M. G. Kanatzidis, A. Facchetti and T. J. Marks, *J. Am. Chem. Soc.*, 2010, **132**, 10352–10364.
14 C. Y. Advanced MaterialsKoo, K. Song, Y. Jung, W. Yang, S. H. Kim, S. Jeong and J. Moon, *ACS Appl. Mater. Interfaces*, 2012, **4**, 1456–1461.
15 W. T. Park, I. Son, H. W. Park, K. B. Chung, Y. Xu, T. Lee and Y. Y. Noh, *ACS Appl. Mater. Interfaces*, 2015, **7**, 13289–13294.
16 J. Zha and H. Roggendorf, *Adv. Mater.*, 1991, **3**, 522.
17 Y. Aoki, T. Kunitake and A. Nakao, *Chem. Mater.*, 2005, **17**, 450–458.
18 I. Ichinose, H. Senzu and T. Kunitake, *Chem. Mater.*, 1997, **9**, 1296–1298.
19 J. Park, T. Gergely, Y. S. Rim and S. Pyo, *ACS Appl. Electron. Mater.*, 2019, **1**, 505–512.
20 K. K. Banger, R. L. Peterson, K. Mori, Y. Yamashita, T. Leedham and H. Sirringhaus, *Chem. Mater.*, 2014, **26**, 1195–1203.
21 Y. H. Kang, K. S. Jang, C. Lee and S. Y. Cho, *ACS Appl. Mater. Interfaces*, 2016, **8**, 5216–5223.
22 H. Pu, Q. Zhou, L. Yue and Q. Zhang, *Semicond. Sci. Technol.*, 2013, **28**, 105002.
23 J. Xu, Y. Wang, H. Shan, Y. Lin, Q. Chen, V. A. Roy and Z. Xu, *ACS Appl. Mater. Interfaces*, 2016, **8**, 18991–18997.
24 M. Eslamian, *Prog. Org. Coat.*, 2017, **113**, 60–73.
25 M. Souada, C. Louage, J. Y. Doisy, L. Meunier, A. Benderrag, B. Ouddane, S. Bellayer, N. Nuns, M. Traisnel and U. Maschke, *Ultrason. Sonochem.*, 2018, **40**, 929–936.
26 G. Huang, L. Duan, Y. Zhao, G. Dong, D. Zhang and Y. Qiu, *Appl. Phys. Lett.*, 2014, **105**, 122105.
27 P. K. Nayak, M. N. Hedhili, D. Cha and H. N. Alshareef, *ACS Appl. Mater. Interfaces*, 2013, **5**, 3587–3590.
28 X. Yang, S. Jiang, J. Li, J.-H. Zhang and X.-F. Li, *RSC Adv.*, 2018, **8**, 20990–20995.
29 S.-J. Seo, C. G. Choi, Y. H. Hwang and B.-S. Bae, *J. Phys. D: Appl. Phys.*, 2009, **42**, 035106.
30 C.-G. Lee and A. Dodabalapur, *Appl. Phys. Lett.*, 2010, **96**, 243501.
31 P. Barquinha, A. Pimentel, A. Marques, L. Pereira, R. Martins and E. Fortunato, *J. Non-Cryst. Solids*, 2006, **352**, 1756–1760.
32 Y. Jeong, C. Bae, D. Kim, K. Song, K. Woo, H. Shin, G. Cao and J. Moon, *ACS Appl. Mater. Interfaces*, 2010, **2**, 611–615.
33 L.-C. Liu, J.-S. Chen and J.-S. Jeng, *Appl. Phys. Lett.*, 2014, **105**, 023509.
34 J.-S. Jeng, *J. Alloys Compd.*, 2016, **676**, 86–90.
35 Y. S. Rim, D. L. Kim, W. H. Jeong and H. J. Kim, *Appl. Phys. Lett.*, 2010, **97**, 233502.
36 K. Kishimoto, Y. Nose, Y. Ishikawa, M. N. Fujii and Y. Uraoka, *J. Alloys Compd.*, 2016, **672**, 413–418.
37 B. M. Teo, S. W. Prescott, M. Ashokkumar and F. Grieser, *Ultrason. Sonochem.*, 2008, **15**, 89–94.

Open Access Article. Published on 28 July 2020. Downloaded on 8/15/2024 10:14:40 PM.
This article is licensed under a Creative Commons Attribution-NonCommercial 3.0 Unported Licence.

38 M. Lim, Y. Son and J. Khim, *Ultrason. Sonochem.*, 2011, **18**, 460–465.
39 A. Li, R. Zhong, X. Li and J. Zhang, *Chem. Eng. Process.*, 2020, **150**, 107884.
40 A. Liu, G. X. Liu, F. K. Shan, H. H. Zhu, S. Xu, J. Q. Liu, B. C. Shin and W. J. Lee, *Curr. Appl. Phys.*, 2014, **14**, S39–S43.
41 K. Umeda, T. Miyasako, A. Sugiyama, A. Tanaka, M. Suzuki, E. Tokumitsu and T. Shimoda, *J. Appl. Phys.*, 2013, **113**, 184509.
42 A. T. Oluwabi, A. Katerski, E. Carlos, R. Branquinho, A. Mere, M. Krunks, E. Fortunato, L. Pereira and I. Oja Acik, *J. Mater. Chem. C*, 2020, **8**, 3730–3739.
43 Y. Liang, J. Yong, Y. Yu, A. Nirmalathas, K. Ganesan, R. Evans, B. Nasr and E. Skafidas, *ACS Nano*, 2019, **13**, 13957–13964.
44 J. Yang, B. Wang, Y. Zhang, X. Ding and J. Zhang, *J. Mater. Chem. C*, 2018, **6**, 12584–12591.
45 M. N. Le, H. Kim, Y. K. Kang, Y. Song, X. Guo, Y.-G. Ha, C. Kim and M.-G. Kim, *J. Mater. Chem. C*, 2019, **7**, 10635–10641.

This journal is © The Royal Society of Chemistry 2020